arXiv:astro-ph/0107295v1 16 Jul 2001

Discovery of the Galaxy Proximity Effect and Implications for Measurements of the Ionizing Background Radiation at Low Redshifts

Sebastian M. Pascarelle, Kenneth M. Lanzetta, & Hsiao-Wen Chen[1]
Department of Physics and Astronomy, State University of New York at Stony Brook
Stony Brook, NY 11794-3800, U.S.A.

and

John K. Webb
School of Physics, University of New South Wales
Sydney, NSW 2052, AUSTRALIA

ABSTRACT

We present an analysis of galaxy and QSO absorption line pairs toward 24 QSOs at redshifts between $z \approx 0.2$ and 1 in an effort to establish the relationship between galaxies and absorption lines in physical proximity to QSOs. We demonstrate the existence of a *galaxy* proximity effect, in that galaxies in the vicinities of QSOs do not show the same incidence and extent of gaseous envelopes as galaxies far from QSOs. We show that the galaxy proximity effect exists to galaxy–QSO velocity separations of $\simeq 3000$ km s^{-1}, much larger than the size of a typical cluster ($\simeq 1000$ km s^{-1}), *i.e.* it is more comparable to the scale of the sphere of influence of QSO ionizing radiation rather than the scale of galaxy–QSO clustering. This indicates that the QSO ionizing radiation rather than some dynamical effect from the cluster environment is responsible for the galaxy proximity effect. We combine previous findings that (1) many or most Lyα absorption lines arise in extended galaxy envelopes, and (2) galaxies cluster around QSOs to show that the magnitude of the Lyα forest proximity effect is underestimated. Consequently, determinations of the UV ionizing background intensity using the proximity effect are likely overestimated. We use the galaxy–QSO cross-correlation function measured from our data to estimate the magnitude of this overestimate and find that it could be as high as a factor of 20 at $z \lesssim 1$. This can have strong implications for models of the origin and

---

[1] Current address: The Observatories of the Carnegie Institution of Washington, 813 Santa Barbara Street, Pasadena, CA 91101, U.S.A. E-Mail: hchen@ociw.edu

evolution of the ionizing background, and may indicate that QSOs produce sufficient ionizing flux at all redshifts to account for the entire background radiation field.

Subject headings: quasars: absorption lines—cosmology: diffuse radiation

1. Introduction

The forest of Lyα absorption lines identified in the spectra of QSOs probes physical conditions of the universe at redshifts ranging through $z \approx 5$. Previous studies have established the redshift distribution $n(z)$ of Lyα-forest absorption lines, with two primary results: First, $n(z)$ generally increases with increasing redshift according to a power-law relation $n(z) \propto (1+z)^{\gamma}$, where γ ranges from $\gamma = 0.1$ to 0.5 at redshifts $z \lesssim 1.5$ up to $\gamma = 1.85$ to 2.78 at redshifts $z \approx 1.5 - 4$ (Lu, Wolfe, & Turnshek 1991, hereafter LWT91; Kulkarni & Fall 1993, hereafter KF93; Bechtold 1994, hereafter B94; Bahcall et al. 1996; Giallongo et al. 1996; Kim et al. 1997; Weymann et al. 1998; Savaglio et al. 1999). Second, $n(z)$ decreases with increasing redshift along individual lines of sight at redshifts near the emission redshifts of the QSOs (Weymann, Carswell, & Smith 1981; Carswell et al. 1982; Murdoch et al. 1986; Tytler 1987; Bajtlik, Duncan, & Ostriker 1988, hereafter BDO88; LWT91; KF93; B94; Cooke, Espey, & Carswell 1997). This latter effect is known as the "proximity effect" and is generally believed to exist because absorbers near QSOs (which are subject to ionizing radiation from the background radiation field and from the QSOs) are more highly ionized than absorbers far from QSOs (which are subject to ionizing radiation from only the background radiation field) and so on average exhibit smaller neutral hydrogen column densities and weaker Lyα absorption lines (BDO88).

The primary utility of the proximity effect is that it is sensitive to the intensity of the background ionizing radiation field. Under an assumption of ionization equilibrium, the deficit of Lyα absorption lines (with respect to an extrapolation of the general cosmological trend) at redshifts near the emission redshift of a QSO depends on the ratio of the flux of ionizing photons from the QSO to the mean intensity of ionizing photons from the background ionizing radiation field. Measurement of the proximity effect fixes this ratio, and measurement of the QSO spectral energy distribution fixes the flux of ionizing photons from the QSO, thus allowing the intensity of ionizing photons from the background ionizing radiation field to be directly inferred. Results are usually expressed in terms of the mean specific intensity of the background ionizing radiation field at the Lyman limit, $J_{\nu_{\rm LL}}$.

Knowledge of $J_{\nu_{\rm LL}}$ as a function of redshift is crucial for understanding galaxies, because ionizing radiation directly affects processes of star and galaxy formation. A higher level of $J_{\nu_{\rm LL}}$ at high redshifts would have increased the ionization fraction of the universe, preventing gas from collapsing down to form clouds, and consequently delaying or hampering star formation activity to later times (*e.g.*, Dekel & Rees 1987; Efstathiou 1992). Various groups have applied the proximity effect to measure $J_{\nu_{\rm LL}}$ at both low and high redshifts. At low redshifts ($z \lesssim 1$), the density of Lyα-forest absorption lines is relatively low, and only a single (tentative) measurement of $J_{\nu_{\rm LL}}$ has been made, yielding $J_{\nu_{\rm LL}} \approx 6.0 \times 10^{-24}$ erg s^{-1} cm^{-2} sr^{-1} Hz^{-1} (KF93). At high redshifts ($z \approx 2-4$), the density of Lyα-forest absorption lines is relatively high, and various measurements of $J_{\nu_{\rm LL}}$ in the range $J_{\nu_{\rm LL}} = 0.6 - 3.0 \times 10^{-21}$ erg s^{-1} cm^{-2} sr^{-1} Hz^{-1} have been obtained (BDO88; LWT91; B94; Giallongo et al. 1996e). (For comparison, measurements of $J_{\nu_{\rm LL}}$ from observations of Hα emission of Galactic and intergalactic clouds and photoionization edges of the neutral hydrogen disks of nearby galaxies (*e.g.*, Maloney 1993) typically determine $J_{\nu_{\rm LL}}$ in the range $J_{\nu_{\rm LL}} \approx 1 - 10 \times 10^{-23}$ erg s^{-1} cm^{-2} sr^{-1} Hz^{-1} at redshift $z \sim 0$.)

But previous measurements of $J_{\nu_{\rm LL}}$ from the proximity effect have assumed that the clouds that produce the Lyα forest are uniformly distributed in space, even in the vicinities of QSOs. This assumption may not be valid in light of the following two points: First, direct comparison of galaxy and absorber redshifts along common lines of sight indicates that at least 50%—and possibly all—of Lyα absorbers at redshifts $z \lesssim 1$ are associated with galaxies (Lanzetta et al. 1995, hereafter L95; Chen et al. 1998, hereafter C98). Second, various observations show that galaxies cluster around QSOs (Bahcall, Schmidt, & Gunn 1969; Hartwick & Schade 1990; Bahcall & Chokshi 1991; Fisher et al.1996; Yee & Green 1987; Boyle, Shanks, & Yee 1988). If many or most Lyα absorbers are associated with galaxies, and if galaxies cluster around QSOs, then previous measurements have *underestimated* the magnitude of the proximity effect, or, equivalently, *overestimated* $J_{\nu_{\rm LL}}$ (see also Loeb & Eisinstein 1995). This may have important implications for our understanding of galaxies and of the sources responsible for the background ionizing radiation field.

To address these issues, we use a sample of galaxies and absorbers toward 24 low-redshift ($z \lesssim 1$) QSOs to examine the incidence and extent of gas envelopes around galaxies in the vicinities of QSOs and far from QSOs. We find several main results as follows: First, there exists a *galaxy proximity effect* in that galaxies in the vicinities of QSOs do not exhibit the same incidence and extent of gaseous envelopes as galaxies far from QSOs. Second, the galaxy proximity effect appears to extend to velocity separations from the QSOs of up to ≈ 3000 km s^{-1}, rather than up to only ≈ 1000 km s^{-1}, which suggests that the effect is related to ionizing radiation from the QSOs rather than to the physical environments of the QSOs. Third, the amplitude of the galaxy–QSO cross-correlation function implies that previous measurements have overestimated $J_{\nu_{\rm LL}}$ by a factor of ≈ 20. While a standard Friedmann cosmology with $\Omega = 1$ is assumed throughout, it should be noted that the entire analysis presented in this paper is completely independent of the assumed value of H_0.

In § 2 we present the data set used in our analysis. In § 3 we demonstrate the existence of a galaxy proximity effect from our galaxy-absorber pairs and discuss its origin. In § 4 we calculate the magnitude of the overestimate of the ionizing background radiation intensity $J_{\nu_{\rm LL}}$ derived from the proximity effect, using clustering information derived from the galaxy–QSO cross-correlation function. Finally, we discuss these results in the context of our current understanding of the origin and evolution of $J_{\nu_{\rm LL}}$ in § 5, and describe other effects that also can cause an overestimate.

2. Data

2.1. Galaxies

Observations of galaxies used in the analysis were obtained from a portion of our imaging and spectroscopic survey of faint galaxies in the fields of Hubble Space Telescope (*HST*) spectroscopic target QSOs (L95; Lanzetta, Webb, & Barcons 1996; C98). The goal of the survey is to establish the relationship between galaxies and Lyα absorption systems by directly comparing galaxies and Lyα absorbers along common lines of sight. The survey includes 523 galaxies of magnitude $r \lesssim 22.5$ drawn from within a few arcmin of 24 background QSOs. Redshifts of the galaxies were determined from various ground-based spectroscopic observations, the details of which have been presented elsewhere (L95; Lanzetta, Webb, & Barcons 1996; C98). The galaxy redshifts range from $z = 0.02$ to ~ 1.5, and the galaxy impact parameters to the QSO lines of sight range from $\rho = 11$ to 1430 h^{-1} kpc.

2.2. Absorbers

Observations of absorbers used in the analysis were obtained from the *HST* archive. Specifically, we analyzed Faint Object Spectrograph (FOS) spectra of 24 QSOs of emission redshift $z = 0.20$ to 1.07. First, we searched the QSO spectra for Lyα absorption lines according to a 5σ detection threshold criterion. Next, we searched the QSO spectra for additional Lyα absorption lines from each of the galaxies of the sample according to a 3σ detection threshold criterion (L95). We included upper limits of equivalent width $W < 0.35$ Å for galaxies for which no Lyα absorption lines were measured in the QSO spectra.

Using these criteria, we identified a total of 229 Lyα absorption lines in the spectra of the 24 QSOs. All absorbers included in our study have a neutral hydrogen column density $N(\mathrm{H\,I}) > 10^{14}$ cm^{-2}. It has been found that more than 75% of these are contaminated by C IV (Songaila & Cowie 1996), and such Lyα absorbers are found to be strongly clustered (Fernandez-Soto et al.1996). Therefore, it follows that these absorbers are most likely to arise in galaxies at high redshifts.

The equivalent width sensitivities of the spectra vary significantly, both from spectrum to spectrum and within individual spectra. To account for these variations, we measured the equivalent width sensitivity versus wavelength of all QSOs in the sample, based on polynomial fits to the spectra and noise spectra. In this way, we employed a uniform equivalent width sensitivity criterion across the spectra.

2.3. Galaxy and Absorber Pairs

A total of 258 of the galaxies of the sample either (1) produce a detected Lyα absorption line or (2) do not produce an absorption line to within a 3σ limiting equivalent width threshold of 0.35 Å. The remaining galaxies have redshifts which either are larger than the redshift of the background QSO or would place the Lyα absorption line in a wavelength region of the QSO spectrum with an equivalent width sensitivity above the 3σ limiting threshold criterion.

We established galaxy and absorber pairs using the galaxy–absorber cross-correlation function $\xi_{ga}(\Delta v, \rho)$ measured by Lanzetta et al.(1997, 2001) on the basis of 3125 galaxy and absorber pairs. Specifically, following Chen et al. 1998 we formed galaxy and absorber pairs by requiring that (1) $\xi_{ga}(\Delta v, \rho) > 1$ and (2) $\rho < 200\ h^{-1}$ kpc. If more than one galaxy satisfied these criteria for a given absorption system, we ascribed the galaxy with the smallest impact parameter to form the pair. In total, we identified 73 galaxy-absorber pairs and 151 galaxies that do not produce Lyα absorption to within sensitive upper limits. Detailed information about each of the fields studied, including coordinates of the QSOs, emission redshifts, and spectral indices, and numbers of absorbers and galaxies in the field is given in Table 1.

3. The Galaxy Proximity Effect

Previous work by Lanzetta et al.(1995) and Chen et al.(1998) has demonstrated a distinct anticorrelation between Lyα absorption line equivalent width W and galaxy impact parameter ρ at redshifts $z \lesssim 1$ for intervening galaxies far from the vicinities of background QSOs (with a line-of-sight velocity difference $\Delta v \gtrsim 3000$ km s^{-1}). In simplest terms, galaxies at impact parameters $\rho \lesssim 180\ h^{-1}$ kpc are *almost always* associated with corresponding Lyα absorption lines, while galaxies at larger impact parameters rarely are. This result is shown in the top left panel of Figure 1, which plots the logarithm of W versus the logarithm of ρ. (Figure 1 contains data from an additional 14 QSO fields not included in the earlier studies, bringing the total number of fields studied to 24.) On the basis of 66 galaxy and absorber pairs and 91 galaxies that do not produce corresponding Lyα absorption to within sensitive upper limits, we find according to the generalized Kendall test that Lyα absorption equivalent width is anti-correlated with galaxy impact parameter at the 7σ level of significance. Specifically, in the top left panel of Figure 1 there are 57 galaxies with impact parameters $\rho \leq 180\ h^{-1}$ kpc, and 45 of these (79%) are associated with corresponding Lyα absorption lines, while there are 100 galaxies with impact parameters $\rho > 180\ h^{-1}$ kpc, and only 21 of these (21%) are associated with detectable absorption lines to within sensitive upper limits.

The sample of galaxies discussed here and presented in the top left panel of Figure 1 are sufficiently displaced from the background QSOs that they lack any physical association with the QSOs, *i.e.*, there are no dynamical or radiative processes arising from the QSOs that directly affect the galaxies. But how do the absorption properties differ for galaxies in physical proximity to the background QSOs? Can the tenuous galaxy envelopes survive the intense ionizing radiation from the QSO and/or the dynamical effects of the QSO cluster environment? If galaxies near QSOs lack the same absorption properties as galaxies far from QSOs, one has to distinguish between dynamical effects such as tidal stripping, which might exist in the cluster environment, and radiation effects, such as the increased amount of ionizing radiation from the QSOs relative to the background radiation field. In an effort to make this distinction, we have created four subsamples from our data set in order to examine the incidence and extent of the gaseous envelopes of galaxies at various velocity separations from the background QSOs. These subsamples are (1) the "near" subsample, consisting of galaxies near enough to the QSOs to be affected by the ionizing radiation of the QSOs, (2) the "far" subsample, presented in the top left panel of Figure 1, consisting of galaxies far enough from the QSOs to lie outside the range of the ionizing radiation of the QSOs, (3) the "cluster" subsample, consisting of galaxies within what we define as the cluster environment, and (4) the "intermediate" subsample, consisting of galaxies outside the cluster environment but still subject to effects of the ionizing radiation of the QSOs. These are described in detail in the following sections.

3.1. Extent of QSO Ionizing Radiation Field

The control sample for this analysis is the sample of galaxies presented in the top left panel of Figure 1, which we call the "far" subsample. It contains galaxies which are sufficiently far from the background QSOs so as to be considered completely outside the effects of the QSO radiation. To define the extent of the QSO radiation field we must determine the radius at which the QSO radiation is exactly balanced by the background radiation field. We can think of the ionizing radiation emitted by the QSO as forming a "sphere of influence" whose size depends on the relative strength of this radiation in comparison to the diffuse ionizing background radiation field. A measure of this relative strength is given by the ratio of the QSO ionization rate to the background ionization rate,

$$\omega(z) = \left(\int_{\nu_{\rm LL}}^{\infty} \frac{F_\nu^Q \sigma_\nu}{h\nu} d\nu\right) \bigg/ \left(\int_{\nu_0}^{\infty} \frac{4\pi J_\nu \sigma_\nu}{h\nu} d\nu\right) f(z) \tag{1}$$

where

$$f(z) = \frac{(1+z)^5}{(1+z_q)} \left[\frac{(1+z_q)^{0.5} - 1}{(1+z_q)^{0.5} - (1+z)^{0.5}}\right]^2 \tag{2}$$

for $\Omega = 1$. Here, F_ν^Q is the flux density of the QSO, J_ν is the specific intensity of the ionizing background radiation field, σ_ν is the absorption cross section of neutral hydrogen gas, $\nu_{\rm LL}$ is the observed Lyman limit frequency at the redshift of the galaxy, and ν_0 is the restframe Lyman limit frequency. The cosmological factors are contained in $f(z)$, where z is the redshift of the galaxy and z_q is the redshift of the QSO.

To evaluate equation (1), it is first necessary to measure the spectral energy distributions of the QSOs and their flux densities at the Lyman limit. First, we created a final spectrum of each QSO by patching together the highest signal-to-noise parts of the various FOS observations obtained through different gratings, which in most cases covered rest-frame wavelengths $\lambda \approx 1000$ to 2000 Å. Next, we identified regions of continuum by selecting portions of the QSO spectra likely to be free of the many Fe II multiplets and other prominent emission features according to the composite QSO spectrum of Francis et al.(1991). Finally, we measured the best-fit spectral index α and Lyman limit flux density F_0 of each QSO by fitting a power-law model to the selected wavelength regions of the spectrum assuming $F_\nu^Q = F_0(\nu/\nu_0)^\alpha$, where ν_0 is the frequency corresponding to the Lyman limit.

We then evaluated the integrals in equation (1), assuming first that J_ν may be approximated by $J_\nu = J_0(\nu/\nu_0)^\beta$, where $J_0 = 1.0 \times 10^{-23}$ erg s^{-1} cm^{-2} sr^{-1} Hz^{-1} (KF93) and β is the background spectral index estimated from a fit to the range of β (for a background arising primarily from QSOs) given in M92 for $z = 0 - 1$, and that the H I cross section is very well approximated by $\sigma \simeq \sigma_0(\nu/\nu_0)^{-3}$ (Osterbrock 1989). The resulting simplified version of equation (1) is

$$\omega(z) = \frac{F_0(z)\nu_{\rm LL}^{\alpha-3}}{J_0(z)\nu_0^{\beta-3}} \frac{\beta-3}{\alpha-3} f(z). \tag{3}$$

The extent of the QSO ionizing radiation sphere of influence, and thus the dividing line between the "near" and "far" subsamples, is defined to be the point where ionization due to the QSO is exactly balanced by ionization due to the background radiation field, i.e., where $\omega(z)$ is unity. We measured $\omega(z)$ using equation (3) for all galaxy-absorber pairs in our sample, and Figure 2 shows a plot of log $\omega(z)$ versus log Δv (galaxy–QSO velocity separation). It can be seen from Figure 2 that, while there is an obvious spread in log $\omega(z)$ due to the various QSO radiation intensities, a mean value of log $\omega(z) = 0$ at log $\Delta v = 3.477$ km s^{-1} ($\Delta v = 3000$ km s^{-1}) fits quite well and different values of J_0 than the adopted 10^{-23} erg s^{-1} cm^{-2} sr^{-1} Hz^{-1} would have little consequence in the determination of subsamples. In addition, adopting a different cosmological model such as LCDM would only change the calculation of $f(z)$ in our entire analysis. We find that the difference in $f(z)$ between SCDM and LCDM would amount to no more than a factor of two at $z \lesssim 1$. Because of the small negative slope shown in Figure 2, the difference in $f(z)$ would have little effect in the determination of subsamples. The results of our analysis are therefore sensitive to neither the adopted cosmological model, nor the assumed J_0.

We find that galaxies at velocity separations $\Delta v < 3000$ km s^{-1} from the background QSOs in our sample are likely to be affected by the enhanced ionizing radiation from the QSOs, while galaxies at greater velocity separations are subject only to the effects of the background ionizing radiation field. Using this information, we created the "near" subsample of galaxies, which have velocity separations $\Delta v < 3000$ km s^{-1}, and the "far" subsample, which have velocity separations $\Delta v > 3000$ km s^{-1}.

3.2. Galaxy–QSO Cross-Correlation Function

To establish the "cluster" and "intermediate" subsamples, we must determine a "dynamical scale" over which the galaxies of this study cluster around the QSOs of this study. We measured the galaxy–QSO cross-correlation function $\xi_{gq}(\Delta v)$ in terms of galaxy–QSO velocity separation Δv, which is shown in Figure 3. There is a prominent peak at $\Delta v \simeq 0$, which indicates that the galaxies do indeed cluster around the QSOs. We fit the cross-correlation function with a Gaussian model, which yielded FWHM = 1170 km s^{-1}. We take galaxies to be within the cluster environment if they occur at velocity separations at which the galaxy–QSO cross-correlation function exceeds unity [i.e. $\xi_{\rm gq}(\Delta v) > 1$] in Figure 3. According to the Gaussian fit of $\xi_{\rm gq}(\Delta v)$, the clustering environment extends to $\Delta v = \pm 1180$ km s^{-1}. Therefore, galaxies with $-1180 < \Delta v < 1180$ are susceptible to the dynamical effects of the cluster environment, and we define this subsample as the "cluster" subsample. Galaxies with $1180 < \Delta v < 3000$ km s^{-1} are designated as the "intermediate" subsample, since they occur outside the clustering environment but are still susceptible to the effects of the QSO ionizing flux.

3.3. Statistical Analysis

We defined in the previous sections four subsamples as follows: (1) the "near" subsample containing galaxies with $\Delta v < 3000$ km s^{-1}, (2) the "far" subsample containing galaxies with $\Delta v > 3000$ km s^{-1}, (3) the "cluster" subsample containing galaxies with $|\Delta v| < 1180$ km s^{-1}, and (4) the "intermediate" subsample containing galaxies with $1180 < \Delta v < 3000$ km s^{-1}. The next step is then to compare the W (equivalent width) versus ρ (impact parameter) relation for each subsample to determine whether or not the absorption properties of galaxies vary among the subsamples. A detailed statistical analysis was carried out to perform this comparison. We used Gehan (Gehan 1965) and Log-rank (Mantel 1966; Cox 1972) tests for incomplete observations, modified for application to multivariate observations (Wei & Lachin 1984). These tests are a generalized version of the Kolmogorov-Smirnov test designed to properly take into account the existence of arbitrarily censored (or failed) observations. The purpose of these tests is to examine the probability of the null hypothesis, *i.e.*, that any two subsamples are drawn from the same parent sample; the tests are χ^2 distributed with respect to the null hypothesis. In our case, the test results will determine whether galaxies in the different subsamples share common physical properties of extended gas on the basis of the W versus ρ relation. As mentioned earlier, we adopt the far subsample as the control sample and compare the other three subsamples.

In making these comparisons, we must take into account the peculiar motions of galaxies induced by the cluster environment (Loeb & Eisenstein 1995; also, *c.f.* Figure 3). Some fraction of the galaxies in both the cluster subsample and the near subsample that do not produce absorption lines can actually lie behind the QSO due to these peculiar motions. To account for this, we selected from our subsamples non-absorbing galaxies that lie within the cluster environment ($|\Delta v| < 1180$ km s^{-1}) and randomly placed them either in front of or behind the QSO when calculating the Gehan and Log-rank statistics. This process was repeated 100 times, and a probability was calculated for the average statistics of all 100 runs.

The results are given in Table 2 and illustrated in Figure 1, which shows W versus ρ for galaxies in all the subsamples. On the basis of Figure 1 it appears that the Lyα absorption properties of galaxies in the near sample are utterly unlike the Lyα absorption properties of galaxies in the far sample. For example, in the far sample, galaxies at impact parameters $\rho < 100\ h^{-1}$ kpc are *almost always* associated with corresponding Lyα absorption lines (30 of 32 cases), whereas in the near sample, galaxies at impact parameters $\rho < 100\ h^{-1}$ kpc are *almost never* associated with corresponding Lyα absorption lines (4 of 22 cases). Apparently, *the only place that galaxies close to the lines of sight to background QSOs are not associated with corresponding* Lyα *absorption lines is in the immediate vicinities of the QSOs.*

The statistical significance of this result is summarized in Table 2, which indicates that the null hypothesis (i.e. that the absorption properties of galaxies in the vicinities of QSOs are identical to the absorption properties of galaxies far from QSOs) can be rejected for all three of the other subsamples in comparison to the far subsample. This can also be seen in the bottom two panels of Figure 1, which show no correlation. Evidently, the anticorrelation between W and ρ that is seen in the far subsample does not exist in *any* of the other subsamples. This indicates two things: (1) there exists a *galaxy proximity effect*, in that galaxies in the vicinities of QSOs do not exhibit the same incidence and extent of gaseous envelopes as galaxies far from QSOs, and (2) this galaxy proximity effect is likely due to the increased level of ionizing radiation from the QSOs above the mean intensity of background ionizing radiation. If the galaxy proximity effect instead arose from some dynamical process induced by the cluster environment in which galaxies were stripped of their H I envelopes (*e.g.*, Morris et al.1993), then there should be a non-negligible probability of the null hypothesis for the intermediate subsample, since these galaxies are outside the cluster environment. Instead, Table 2 shows a vanishingly small probability for all the subsamples, so that the galaxy proximity effect probably exists at all velocity separations out to $\Delta v \simeq 3000$ km s^{-1}, well outside the cluster environment.

We repeated the statistical tests for subsamples in which the dividing line between the intermediate and far subsamples was varied slightly (from $\Delta v = 3000$ km s^{-1} up to $\Delta v = 4200$ km s^{-1}to account for the effect of different cosmological models), and for samples in which the clustering size was varied slightly (from $\Delta v = \pm 600$ km s^{-1} up to $\Delta v = \pm 2000$ km s^{-1}) and found that the main results are insensitive to small variations around the values determined in this paper.

4. Effects of Galaxy Clustering on the Proximity Effect

Results of the previous section suggest that the deficit of absorption lines seen in close proximity to the background QSO (the proximity effect as discussed in §1) has been *underestimated* since the existence of an excess of galaxies near the QSO has been neglected. Therefore, a determination of the mean intensity of the ionizing background radiation field $J_{\nu_{\rm LL}}$ from the proximity effect would be *overestimated*. This implies that all previous estimates of $J_{\nu_{\rm LL}}$ at various redshifts using the proximity effect may have also been overestimated. To determine the magnitude of this overestimate from our data set, we start by following the definition of the proximity effect presented in BDO88.

We first model the observed number of absorption lines per unit redshift with equivalent width above a fixed threshold as a power law of the form

$$n(z) = A_0(1+z)^{\gamma} \tag{4}$$

where A_0 is a normalization constant and γ has been found to range from $\lesssim$0.3 at redshifts < 1.7 (e.g., Weymann et al.1998) to ~ 2.0 at redshifts between $\sim 2-4$ (e.g., B94).

Next, we describe the H I column density $N_{\rm H\,I}$ for a highly ionized absorber near a QSO as

$$N_{\rm H\,I} = N_0[1+\omega(z)]^{-1} \tag{5}$$

where N_0 is the column density of the absorber in the absence of the QSO and $\omega(z)$ is defined in §3.1. The observed distribution of absorber H I column densities is often given by a power law of the form

$$f(N_{\rm H\,I}) \propto N_{\rm H\,I}^{-\eta} \tag{6}$$

so that the number of absorbers with H I column density above some threshold $N_{\rm thr}$ is

$$n(N_{\rm H\,I} \geq N_{\rm thr}) \propto N_{\rm H\,I}^{-\eta+1} \tag{7}$$

Many absorption system studies have found that $\eta \approx 1.7$ (e.g., Carswell et al.1984; Atwood, Baldwin & Carswell 1985; Rauch et al.1992), which then gives

$$n(N_{\rm H\,I} \geq N_{\rm thr}) \propto N_{\rm H\,I}^{-0.7} \tag{8}$$

Therefore, for a sample of absorbers limited by the observed H I column density, the distribution of absorption lines with redshift given in equation (4) *including* the proximity effect is given by

$$n(z) = A_0(1+z)^{\gamma}[1+\omega(z)]^{-0.7} \tag{9}$$

However, given that most of the absorption lines in our sample are associated with galaxies and that galaxies cluster around QSOs, the actual number of potential absorbers must be higher by some factor $\delta_{\rm cl}$, which is the galaxy overdensity in the vicinities of QSOs. So the corrected version of equation (9) is

$$n(z) = A_0(1+z)^{\gamma}[1+\omega_{\rm cl}(z)]^{-0.7}\delta_{\rm cl} \tag{10}$$

Equating equation (9) to equation (10) and collecting terms, we get

$$\left[\frac{1+\omega(z)}{1+\omega_{\rm cl}(z)}\right]^{-0.7} = \delta_{\rm cl} \tag{11}$$

and since the clustering scale ($\simeq$ 1180 km s^{-1}) is smaller than the extent of the proximity effect ($\simeq$ 3000 km s^{-1}), $\omega(z)$ will always be $\gg 1$ so that

$$\left[\frac{\omega(z)}{\omega_{\rm cl}(z)}\right]^{-0.7} = \delta_{\rm cl} \tag{12}$$

Thus, the amount by which the proximity effect has been underestimated is given by

$$\frac{\omega_{\rm cl}(z)}{\omega(z)} = \delta_{\rm cl}^{1.4} \tag{13}$$

To determine the overdensity of galaxies around the QSOs $\delta_{\rm cl}$, we calculated the ratio of the mean number of galaxies per unit velocity separation at $|\Delta v| < 1180$ km s^{-1} to the mean number of galaxies per unit velocity separation at $3000 < \Delta v < 50,000$ km s^{-1}. We find from this ratio that the magnitude of the excess of galaxies in the vicinities of the QSOs is $\delta_{\rm cl} = 8.5$. According to equation (13), then, the proximity effect measured at low redshifts from a sample similar to the one presented in this paper may be underestimated by a factor of 20. Consequently, the strength of the ionizing background radiation field $J_{\nu_{\rm LL}}$ deduced from such a measurement would be overestimated by a factor of 20.

5. Discussion

5.1. Comparison of Local Estimates of $J_{\nu_{\rm LL}}$

A quantitative understanding of the intensity of the ionizing background radiation, $J_{\nu_{\rm LL}}$, as a function of redshift is crucial for models of galaxy formation and evolution, because the ionizing background radiation directly modulates star formation at all redshifts. Unfortunately, it is not possible to measure $J_{\nu_{\rm LL}}$ directly, since the Galaxy is optically thick to ionizing radiation below the Lyman limit. Therefore, we must rely on more indirect means such as measuring its effects on detectable gas outside the Galaxy. At high redshifts ($z \simeq 2 - 4$) our knowledge of $J_{\nu_{\rm LL}}$ comes entirely from detections of the proximity effect (*e.g.*, BDO88, LWT91, B94) and model calculations based on the observed QSO redshift distribution (*e.g.*, M92), which tend to agree that $J_{\nu_{\rm LL}} \simeq 1 \times 10^{-21}$ erg s^{-1} cm^{-2} sr^{-1} Hz^{-1}. Due to the lower density of Lyα absorption lines at low redshifts ($z \lesssim 1$) as compared to high redshifts, detection of the proximity effect at low redshifts is very difficult. Consequently, only a single tentative measurement of the ionizing background has been reported from the proximity effect at $z \sim 0.5$ of $J_{\nu_{\rm LL}} = 0.2 - 3.6 \times 10^{-23}$ erg s^{-1} cm^{-2} sr^{-1} Hz^{-1} (KF93). At these redshifts, however, various other techniques can be used to place constraints on $J_{\nu_{\rm LL}}$ in addition to the proximity effect. In the following, we discuss these various techniques and their results to better depict the redshift evolution of $J_{\nu_{\rm LL}}$ in the context of our results.

There exist several estimates of $J_{\nu_{\rm LL}}$ in the local universe using techniques other than the proximity effect. Since many of these invariably rely on some set of model assumptions, they provide only upper or lower limits rather than specific measurements. For example, observations of a sharp cutoff in the surface density of H I in the outer disks of nearby galaxies can constrain $J_{\nu_{\rm LL}}$ (Bochkarev & Sunyaev 1977). Typical estimates lie in the range $J_{\nu_{\rm LL}} \sim 1 - 10 \times 10^{-23}$ erg s^{-1} cm^{-2} sr^{-1} Hz^{-1}, with the range of values dictated mainly by the assumed structure of the galactic disks (Corbelli & Salpeter 1993; Maloney 1993; Dove & Shull 1994). Uncertainty in the total H I distribution at large radii also adds to the error in such measurements.

Another technique comes from the non-detection of Hα emission from H I clouds. An upper limit of $J_{\nu_{\rm LL}} \lesssim 2 \times 10^{-22}$ erg s^{-1} cm^{-2} sr^{-1} Hz^{-1} was determined from non-detections of Hα emission from high-velocity clouds in the Galaxy halo (Kutyrev & Reynolds 1989; Songaila, Bryant, & Cowie 1989). However, these clouds may be affected by internal sources of ionization and/or be shielded from the intergalactic radiation field. A more reliable measurement can come instead from intergalactic H I clouds. Two independent studies arrived at similar stringent upper limits on $J_{\nu_{\rm LL}}$ ($J_{\nu_{\rm LL}} \lesssim 8 \times 10^{-23}$ erg s^{-1} cm^{-2} sr^{-1} Hz^{-1}) from a lack of Hα emission from several intergalactic clouds (Donahue, Aldering, & Stocke 1995; Vogel et al.1995). Also, observations of extraplanar and outer disk Hα emission from several spiral galaxies place a firm upper limit of $J_{\nu_{\rm LL}} \lesssim 1 \times 10^{-22}$ erg s^{-1} cm^{-2} sr^{-1} Hz^{-1} (Hoopes, Walterbos, & Rand 1999).

Finally, there have been several determinations of $J_{\nu_{\rm LL}}$ based on the QSO luminosity function under the assumption that a dominant fraction of the ionizing flux at low redshift is contributed by QSOs. Typical estimates lie in the range $J_{\nu_{\rm LL}} \sim 2 - 8 \times 10^{-23}$ erg s^{-1} cm^{-2} sr^{-1} Hz^{-1} (Miralda-Escudé & Ostriker 1990; M92; Zuo & Phinney 1993). More recent calculations, taking into account updated knowledge of the observed QSO redshift distribution find $J_{\nu_{\rm LL}} = 0.8 - 2.1 \times 10^{-23}$ erg s^{-1} cm^{-2} sr^{-1} Hz^{-1} (Shull et al.1999). Furthermore, a *lower* limit of $J_{\nu_{\rm LL}} \geq 1 \times 10^{-23}$ erg s^{-1} cm^{-2} sr^{-1} Hz^{-1} was suggested from measurements of the column densities of Fe I, Mg I, Fe II, and Mg II in an intergalactic H I cloud, assuming a QSO-dominated ionizing background (Tumlinson et al.1999). Constraints on $J_{\nu_{\rm LL}}$ from models of the QSO emissivity versus redshift, however, must make assumptions about the local QSO luminosity function, intrinsic QSO spectral shapes, and radiative transfer in the intergalactic medium.

If we take as an acceptable range from the above discussion $J_{\nu_{\rm LL}} \sim 1 - 8 \times 10^{-23}$ erg s^{-1} cm^{-2} sr^{-1} Hz^{-1}, we can see that the KF93 measurement from the proximity effect is quite consistent with these estimates ($J_{\nu_{\rm LL}} = 0.2 - 3.6 \times 10^{-23}$ erg s^{-1} cm^{-2} sr^{-1} Hz^{-1}). If we apply the factor of 20 correction suggested by the results of this paper to the KF93 measurement, the intensity of the ionizing background becomes $J_{\nu_{\rm LL}} = 0.1 - 1.8 \times 10^{-24}$ erg s^{-1} cm^{-2} sr^{-1} Hz^{-1}, almost an order of magnitude weaker than the estimate of Shull et al.(1999). However, these authors have fairly pointed out that their error of $J_{\nu_{\rm LL}}$ was underestimated. Taking a more realistic error estimate, the discrepancy between the two measurements may be reduced to a factor of a few. Because a reduced $J_{\nu_{\rm LL}}$ will result in a smaller ionization correction, the result of our analysis also implies a smaller estimate for Ω_b.

5.2. Sources of the Ionizing Background Radiation

An accurate depiction of the redshift evolution of $J_{\nu_{\rm LL}}$ can also help to constrain the likely candidate sources of the ionizing background radiation, which will in turn have strong consequences on current models of structure formation in the early universe and the collapse and cooling of low-mass objects at early epochs. An obvious source of ionizing radiation is the QSO population. Initially, it was thought that the observed QSO population did not produce enough ionizing photons at high redshifts to satisfy measurements of $J_{\nu_{\rm LL}}$ from the proximity effect, so that there must be other sources such as massive star formation or an undetected QSO population (Miralda-Escudé & Ostriker 1990). Later studies found that indeed QSOs could produce (barely) enough ionizing flux at high redshifts to ionize the universe (Meiksin & Madau 1993), despite the observed decrease in the QSO number density at $z > 3$. Nevertheless, the discovery of metals in high redshift Lyα clouds implies that the intergalactic medium had been contaminated by the products of massive star formation — another viable source of ionizing photons. Coupled with the existence of a large population of star-forming galaxies at $z \sim 3$ reported over the last few years, this implies that ionizing radiation from massive star formation at $z > 3$ can make up for the fraction that QSOs lack (Madau & Shull 1996; Madau, Haardt, & Rees 1999).

However, the high-redshift background ionizing spectrum is dominated by the effects of radiative transfer in a clumpy intergalactic medium, complicating its interpretation. The low-redshift ($z \lesssim 1$) spectrum, on the other hand, should be more representative of its sources. As at higher redshifts, there have been discrepancies at low redshifts between the estimated background flux and the QSO space density, which steeply declines at $z < 2.5$ (Madau 1992, hereafter M92). An underestimate of the proximity effect could then bring the intensity of the ionizing background into closer agreement with current models of QSOs as ionizing sources at low redshift (Giallongo, Fontana, & Madau 1997), especially if this underestimate is as high as a factor of 20.

5.3. Effects of QSO Properties on the Results

The study presented in this paper utilized a randomly selected sample of $z \lesssim 1$ QSOs of various spectral indices and radio properties. Since QSO spectral index and radio power can have an effect on the results of this paper, we discuss each of them here. First, it can be seen from Figure 2 that there is a spread in the value of $\omega(z)$ for a given velocity separation, which implies that there is a spread in QSO ionizing flux density. The velocity separation at which the ionizing flux from the QSO is exactly balanced by the mean intensity of the background ionizing radiation field defines the extent of the proximity effect, and this was found to be $\Delta v \sim 3000$ km s^{-1} from our data. QSOs with larger ionizing flux densities will push the extent of the proximity effect out to larger velocity separations, and QSOs with smaller ionizing flux densities will have a smaller sphere of influence. Therefore, the proximity effect for significantly stronger QSOs will be more severely overestimated due to galaxy clustering than the proximity effect for weaker QSOs (*e.g.*, Loeb & Eisenstein 1995).

Second, while it has been noted that galaxy clustering around low redshift QSOs appears to be independent of QSO radio power for $z < 0.6$, there appears to be a divergence in properties at higher redshifts (Yee & Green 1987). Radio-loud QSOs are often located in rich clusters, while radio-quiet QSOs exist in smaller groups or in the outer regions of clusters. Since most of our QSO sample (15 out of 24) have $z < 0.6$, it is unlikely that radio power has any effect on our conclusions. However, for studies conducted at higher redshifts where the clustering properties vary significantly, the factor of 20 overestimate of $J_{\nu_{\rm LL}}$ calculated in this paper must be adjusted accordingly, since this number directly depends on clustering amplitude. For example, $J_{\nu_{\rm LL}}$ measured from the proximity effect for a sample of radio-loud QSOs at some redshift slightly higher than $z = 0.6$ should be decreased by an additional factor of ~ 4.6 in comparison to a measurement based on radio-quiet QSOs at the same redshift. (Here we assume a typical group has about 20 members and a rich cluster has Abell richness R=1, or about 60 members, so that the correction factor would be $\sim 3^{1.4}$.)

5.4. Additional Contributions to the Overestimate of $J_{\nu_{\rm LL}}$

Galaxy clustering around QSOs is not the only source of error in estimates of $J_{\nu_{\rm LL}}$. The mean intensity of the ionizing background radiation can also be overestimated due to uncertainties in the QSO redshifts (B94). If the QSO emission redshift is measured from broad high-ionization restframe ultraviolet lines such as Lyα or C IV, then velocity shifts with respect to the QSO's systemic redshift will cause estimates of the ionizing background from the proximity effect to be overestimated by factors of $\sim 1.9-2.3$ (McIntosh et al.1999). The low-ionization broad Mg II line, or narrow emission lines such as O II or O III, should instead be used for redshift determinations, since they generally are within ~ 50 km s^{-1} of the QSO systemic velocity. This effect, combined with the effect of galaxy clustering from our study, implies that estimates of the ionizing background from the proximity effect may be overestimated by as much as a factor of ~ 40 if the QSO redshifts come from the broad high-ionization ultraviolet lines. Although most QSO redshifts in our sample have emission redshifts determined from Mg II or O II, there are several that rely only on Lyα and/or C IV, so that this effect should be accounted for even in our data.

Another source of error can come from the assumed slope of the power-law fit to the Lyα absorber column density distribution. In our study, we assumed the widely quoted value $\eta = 1.7$. If, for example, the slope is actually $\eta = 1.5$, as found by Hu et al.(1995), then the overestimate of the ionizing background would increase from a factor of 20 to a factor of 72. For a very steep column density distribution ($\eta = 2.0$) on the other hand, there would still need to be a correction of almost a factor of ten. Thus, measurements of $J_{\nu_{\rm LL}}$ are somewhat sensitive to the assumed slope of the fit to the absorber column density distribution.

The effects discussed here tend to increase the correction factor rather drastically, so that estimates of $J_{\nu_{\rm LL}}$ from the proximity effect may have to be adjusted in some cases by up to a factor of nearly 100. This will have serious consequences on our current understanding of the evolution of $J_{\nu_{\rm LL}}$. In particular, if the differences between local estimates of $J_{\nu_{\rm LL}}$ and estimates at high redshifts are about a factor of ~ 100 as most studies seem to show, then any combination of the effects discussed here could have substantial impact on our understanding of the evolution of $J_{\nu_{\rm LL}}$ by significantly reducing these differences.

6. Summary

To summarize, we have used a sample of Lyα absorption lines and galaxy spectra from 24 low redshift ($z \lesssim 1$) QSO fields to show that there exists a galaxy proximity effect. In other words, galaxies in the vicinities of QSOs do not show the same incidence and extent of gaseous envelopes as galaxies far from QSOs. We find that the scale of the galaxy proximity effect is consistent with the scale of the QSO ionizing radiation field ($\Delta v \lesssim 3000$ km s^{-1}) rather than the scale of galaxy clustering ($\Delta v \lesssim 1180$ km s^{-1}) for our data, indicating that the galaxy proximity effect is due to the increased ionizing radiation from the QSO rather than some cluster environmental effect. We furthermore find that since (1) most Lyα absorption systems arise in galaxies, and (2) galaxies cluster around QSOs, the strength of the proximity effect has likely been underestimated. That is to say, there are more potential Lyα absorbers (galaxies) in the vicinities of QSOs than assumed if clustering is ignored, leading to an underestimate of the magnitude of the proximity effect. Consequently, the mean intensity of the ionizing background radiation $J_{\nu_{\rm LL}}$ as determined from the proximity effect will be overestimated. We find the overestimate to be as high as a factor of 20 at low redshifts (higher if other effects are taken into account), which brings estimates of $J_{\nu_{\rm LL}}$ down to a level which may make it easier to reconcile with models of QSOs as the primary source of ionizing photons.

SMP, HWC, and KML acknowledge support from NASA grant NAGW-4422 and NSF grant AST–9624216. JKW acknowledges support from the Australian Research Council.

REFERENCES

Atwood, B., Baldwin, J. A., & Carswell, R. F. 1985, ApJ, 292, 58

Babul, A., & White, S. D. M. 1991, MNRAS, 253, 31P

Bahcall, J. N., Schmidt, M., & Gunn, J. E. 1969, ApJ, 157, 177

Bahcall, J. N., et al.1996, ApJ, 457, 19

Bahcall, N. A., & Chokshi, A. 1991, ApJ, 380, L9

Bajtlik, S., Duncan, R. C., & Ostriker, J. P. 1988, ApJ, 327, 570 (BDO88)

Bechtold, J. 1994, ApJS, 91, 1 (B94)

Bochkarev, N. G., & Sunyaev, R. A. 1977, Soviet Ast., 21, 542

Boyle, B. J., Shanks, T., & Yee, H. K. C. 1988, in IAU Symp. 130, Large Scale Structures of the Universe, eds J. Audouze, M.-C. Pelletan, & A. Szalay (Dordrecht: Kluwer), 576

Bunker, A. J., Marleau, F. R., & Graham, J. R. 1998, AJ, 116, 2086

Carswell, R. F., Whelan, J. A. J., Smith, M. G., Boksenberg, A., & Tytler, D. 1982, MNRAS, 198,91

Carswell, R. F., Morton, D. C., Smith, M. G., Stockton, A. N., Turnshek, D. A., & Weymann, R. J. 1984, ApJ, 278, 486

Chen H.-W., Lanzetta, K. M., Webb, J. K., & Barcons, X. 1998, ApJ, 498, 77 (C98)

Cooke, A. J., Espey, B., & Carswell, R. F. 1997, MNRAS, 284, 552

Corbelli, E., & Salpeter, E. E. 1993, ApJ, 419, 104

Cox, D. R. 1972, J. Royal Stat. Soc., 34B, 187

Donahue, M., Aldering, G., & Stocke, J. T. 1995, ApJ, 450, L45

Dove, J. B., & Shull, J. M. 1994, ApJ, 423, 196

Fernandez-Soto, A. et al.1996, ApJ, , 460, L85

Fisher, K. B., Bahcall, J. N., Kirhakos, S., & Schneider, D. P. 1996, ApJ, 468, 469

Gehan, E. A. 1965, Biometrika, 52, 203

Giallongo, E., Cristiani, S., D'Odorico, S., Fontana, A., & Savaglio, S. 1996, ApJ, 466, 46

Giallongo, E., Fontana, A., & Madau, P. 1997, MNRAS, 289, 629

Haardt, F. & Madau, P. 1996, ApJ, 461, 20

Hartwick, F. D. A., & Schade, D. 1990, ARA&A, 28, 437

Hoopes, C. G., Walterbos, R. A. M., & Rand, R. J. 1999, ApJ, 522, 669

Hu, E. M., Kim, T.-S., Cowie, L. L., & Songaila, A. 1995, AJ, 110, 1526

Kim, T.-S., Hu, E. M., Cowie, L. L., & Songaila, A. 1997, AJ, 114, 1

Kulkarni, V. P. & Fall, M. 1993, ApJ, 413, L63 (KF93)

Kutyrev, A. S., & Reynolds, R. J. 1989, ApJ, 344, L9

Lanzetta, K. M., Bowen, D. V., Tytler, D., & Webb, J. K. 1995, ApJ, 442, 538 (L95)

Lanzetta, K. M., Webb, J. K., & Barcons, X. 1996, ApJ, 456, 17L

Lanzetta, K. M., Webb, J. K., & Barcons, X. 1997, in Proc. of the 18th Texas Symp. on Relativistic Astrophysics, eds A. Olinto, J. Frieman, & D. Schramm (Dordrecht: Kluwer) 177

Lanzetta, K. M., Webb, J. K., & Barcons, X. 2001, ApJ (in preparation)

Loeb, A. & Eisenstein, D. J. 1995, ApJ, 448, 17

Lu, L., Wolfe, A. M., & Turnshek, D. A. 1991, ApJ, 367, 19 (LWT91)

Madau, P. 1992, ApJ, 389, L1 (M92)

Maloney, P., 1993, ApJ, 414, 98

Mantel, N. 1966, Cancer Chemo. Rep., 50, 690

Martínez, H. J., Merchán, M. E., Valotto, C. A., & Lambas, D. G. 1999, ApJ, 514, 558

McIntosh, D. H., Rix, H.-W., Rieke, M. J., & Foltz, C. B. 1999, ApJ, 517, L73

Miralda-Escudé, J., & Ostriker, J. P. 1990, ApJ, 350, 1

Morris, S. L., Weymann, R. J., Dressler, A., McCarthy, P. J., Smith, B. A., Terrile, R. J., Giovanelli, R., & Irwin, M. 1993, ApJ, 419, 524

Murdoch, H. S., Hunstead, R. W., Pettini, M., & Blades, J. C. 1986, ApJ, 309, 19

Osterbrock, D. E. 1989, in “Astrophysics of Gaseous Nebulae and Active Galactic Nuclei” (Mill Valley, CA: University Science Books) 14

Rauch, M. et al.1992, ApJ, 390, 387

Savaglio, S. et al.1999, ApJ, 515, L5

Sargent, W. L. W., Young, P. J., Boksenberg, A., & Tytler, D. 1980, ApJS, 42, 41

Shaver, P. A., Hook, I. M., Jackson, C. A., Wall, J. V., & Kellermann, K. I. 1999, in “Highly Redshifted Radio Lines,” ASP Conf. Series, Vol. 156, eds C. L. Carilli, S. J. E. Radford, K. M. Menten, & G. I. Langston (Provo, UT: BookCrafters, Inc.) 163

Shull, J. M., Roberts, D., Giroux, M. L., Penton, S. V., & Fardal, M. A. 1999, AJ, 118, 1450

Songaila, A., Bryant, W., & Cowie, L. L. 1989, ApJ, 345, L71

Songaila, A., & Cowie, L. L. 1996, ApJ, 112, 335

Tumlinson, J., Giroux, M. L., Shull, J. M., & Stocke, J. T. 1999, AJ, 118, 2148

Tytler, D. A. 1987, ApJ, 321, 69

Wei, L. J., & Lachin, J. M. 1984, J. Amer. Stat. Assoc., 79, 653

Weymann, R. J., Carswell, R. F., & Smith, M. G. 1981, ARA&A, 19, 41

Weymann, R. J. et al.1998, ApJ, 506, 1

Yee, H. K. C., & Green, R. F. 1987, ApJ, 319, 28

Zuo, L., & Phinney, E. S. 1993, ApJ, 418, 28

This preprint was prepared with the AAS LaTeX macros v4.0.

Fig. 1.— (*top left*) Logarithm of rest-frame equivalent width W versus logarithm of impact parameter ρ plotted for the "far" sample of galaxies, i.e. those galaxies with velocity separations from the background QSOs greater than 3000 km s^{-1}. Open circles with arrows indicated 3σ upper limits to W of 0.35 Å. Note how galaxies at small impact parameters are more likely to produce absorption lines than are galaxies at large impact parameters, and note the marked trend from large W at small ρ to small W at large ρ. (*top right*) Logarithm of rest-frame equivalent width W versus logarithm of impact parameter ρ for the "near" sample of galaxies, i.e. those galaxies with velocity separations from the background QSOs of less than 3000 km s^{-1}. Note how most galaxies in this sample do not produce an absorption line at *any* impact parameter. (*bottom left*) Logright of rest-frame equivalent width W versus logarithm of impact parameter ρ for the cluster subsample of galaxies. (*bottom right*) Logarithm of rest-frame equivalent width W versus logarithm of impact parameter ρ for the intermediate subsample of galaxies.

Fig. 2.— Log $\omega(z)$ versus log Δv for all galaxies–absorber pairs in the data set. The point at which the QSO ionizing radiation is exactly balanced by the diffuse ionizing background radiation field by definition occurs at $\omega = 1$, which corresponds to a galaxy–QSO velocity separation of $\Delta \mathrm{v} = 3000$ km s^{-1} in this plot.

Fig. 3.— The galaxy–QSO cross-correlation function versus galaxy–QSO velocity separation. Note the prominent peak at a velocity separation of zero, indicating that galaxies do indeed cluster around the QSOs. A Gaussian fit to the peak indicates that the typical cluster environment for this sample of galaxies extends out to galaxy–QSO velocity separations of $\approx \pm 1180$ km s^{-1}.

TABLE 1—QSO SAMPLE

QSO Field	RA (J2000)	Dec (J2000)	$z_{\rm em}$	α	$F_0{}^a$	$n_{\rm abs}$	$n_{\rm gxy}$
0044+0303	$00^{\rm h}\,47^{\rm m}\,05^{\rm s}.91$	$+03^\circ19'55''.0$	0.62326	−1.12	0.55	6	5
0122−0021	$01^{\rm h}\,25^{\rm m}\,28^{\rm s}.84$	$-00^\circ05'55''.9$	1.070	−1.55	0.54	20	3
0349−1438	$03^{\rm h}\,51^{\rm m}\,28^{\rm s}.54$	$-14^\circ29'08''.7$	0.61625	−0.58	1.29	5	7
0405−1219	$04^{\rm h}\,07^{\rm m}\,48^{\rm s}.43$	$-12^\circ11'36''.7$	0.57259	−0.71	2.46	15	26
0454−2203	$04^{\rm h}\,56^{\rm m}\,08^{\rm s}.90$	$-21^\circ59'09''.0$	0.53348	−1.05	1.02	15	10
0637−7513	$06^{\rm h}\,35^{\rm m}\,46^{\rm s}.51$	$-75^\circ16'16''.8$	0.656	−1.15	0.64	10	12
0850+4400	$08^{\rm h}\,53^{\rm m}\,34^{\rm s}.20$	$+43^\circ49'01''.0$	0.51390	−0.48	0.37	1	5
0903+1658	$09^{\rm h}\,06^{\rm m}\,31^{\rm s}.92$	$+16^\circ46'12''.8$	0.4121	−0.79	0.10	1	15
1001+2910	$10^{\rm h}\,04^{\rm m}\,02^{\rm s}.63$	$+28^\circ55'35''.5$	0.32970	−0.36	1.31	16	11
1049−0035	$10^{\rm h}\,51^{\rm m}\,51^{\rm s}.50$	$-00^\circ51'16''.6$	0.35990	−1.10	0.81	1	2
1136−1334	$11^{\rm h}\,39^{\rm m}\,10^{\rm s}.70$	$-13^\circ50'43''.5$	0.557	−0.83	0.55	2	13
1216+0657	$12^{\rm h}\,19^{\rm m}\,20^{\rm s}.88$	$+06^\circ38'38''.4$	0.33130	−0.74	1.31	8	11
1259+5920	$13^{\rm h}\,01^{\rm m}\,12^{\rm s}.90$	$+59^\circ02'06''.4$	0.47780	−0.85	1.47	8	17
1317+2743	$13^{\rm h}\,19^{\rm m}\,56^{\rm s}.32$	$+27^\circ28'08''.6$	1.022	−0.48	1.18	38	12
1354+1933	$13^{\rm h}\,57^{\rm m}\,04^{\rm s}.44$	$+19^\circ19'07''.4$	0.719	−1.67	0.69	10	5
1424−1150	$14^{\rm h}\,27^{\rm m}\,38^{\rm s}.17$	$-12^\circ03'50''.6$	0.806	−1.88	0.38	8	8
1545+2101	$15^{\rm h}\,47^{\rm m}\,43^{\rm s}.54$	$+20^\circ52'16''.7$	0.26430	−0.91	0.71	4	7
1622+2352	$16^{\rm h}\,24^{\rm m}\,39^{\rm s}.08$	$+23^\circ45'12''.8$	0.927	−2.23	0.12	12	17
1641+3954	$16^{\rm h}\,42^{\rm m}\,58^{\rm s}.81$	$+39^\circ48'37''.0$	0.59280	−1.57	0.67	2	20
1704+6048	$17^{\rm h}\,04^{\rm m}\,41^{\rm s}.35$	$+60^\circ44'30''.3$	0.37210	−0.83	1.40	13	25
1821+6419	$18^{\rm h}\,21^{\rm m}\,34^{\rm s}.38$	$+64^\circ20'59''.6$	0.2977	−1.17	5.56	13	17
2135−1446	$21^{\rm h}\,37^{\rm m}\,45^{\rm s}.24$	$-14^\circ32'55''.4$	0.20030	−0.23	0.39	5	7
2141+1730	$21^{\rm h}\,43^{\rm m}\,35^{\rm s}.55$	$+17^\circ43'49''.3$	0.21110	−1.38	0.81	1	1
2251+1552	$22^{\rm h}\,53^{\rm m}\,57^{\rm s}.75$	$+16^\circ08'53''.6$	0.859	−2.88	0.74	15	2

[a] 10^{26} erg s^{-1} cm^{-2} Hz^{-1}.

TABLE 2—PROBABILITY OF NULL HYPOTHESIS

Sample	Δv (km s^{-1})	Gehan (%)	Log-rank (%)
near	< 3000	6.5×10^{-5}	7.1×10^{-5}
intermediate	$1180 - 3000$	1.2×10^{-4}	3.0×10^{-3}
cluster	$-1180 - 1180$	6.2×10^{-4}	3.4×10^{-4}

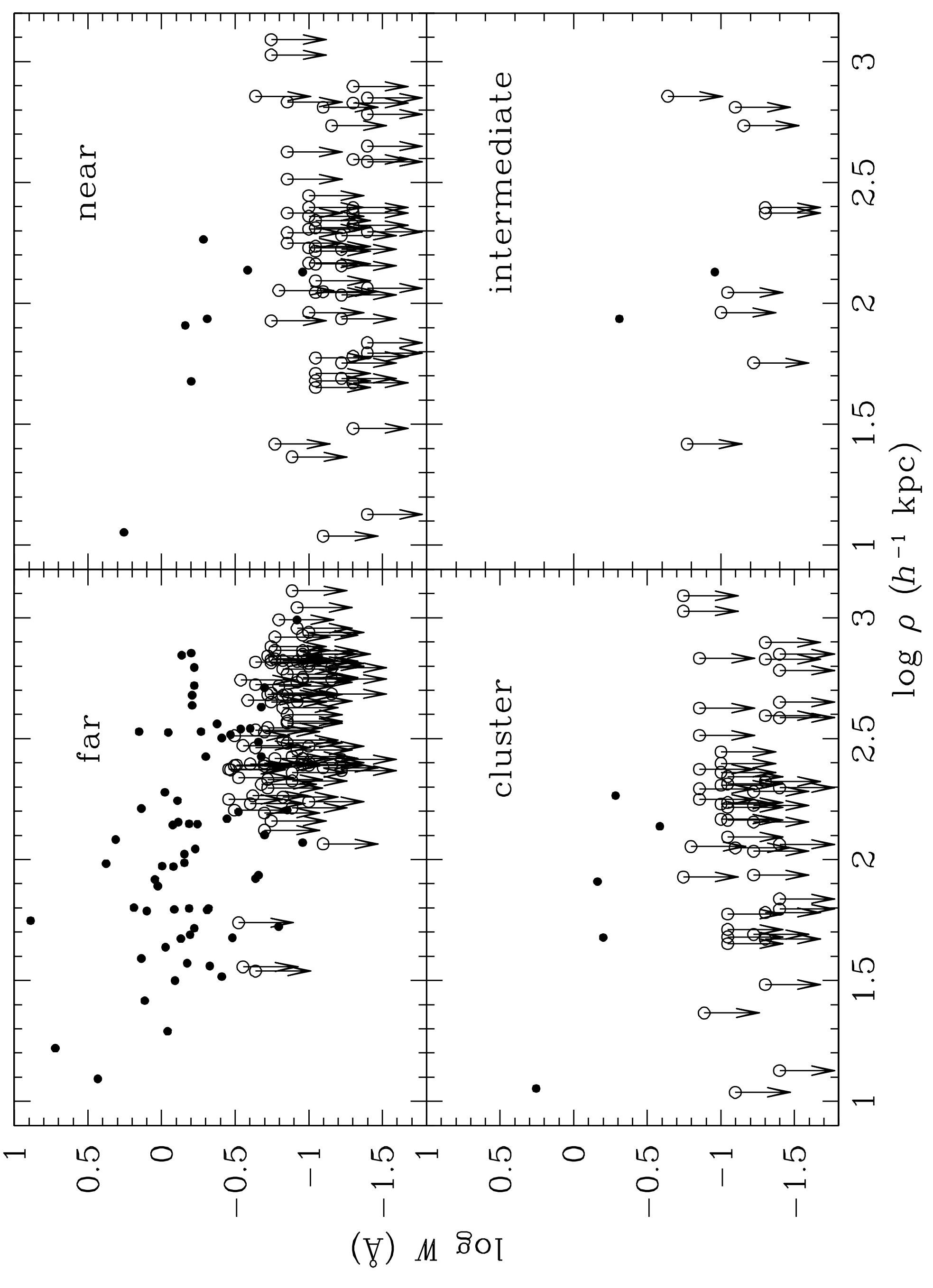
far
near
cluster
intermediate
log W (Å)
log ρ (h^{-1} kpc)
1
0.5
0
−0.5
−1
−1.5
1
1.5
2
2.5
3

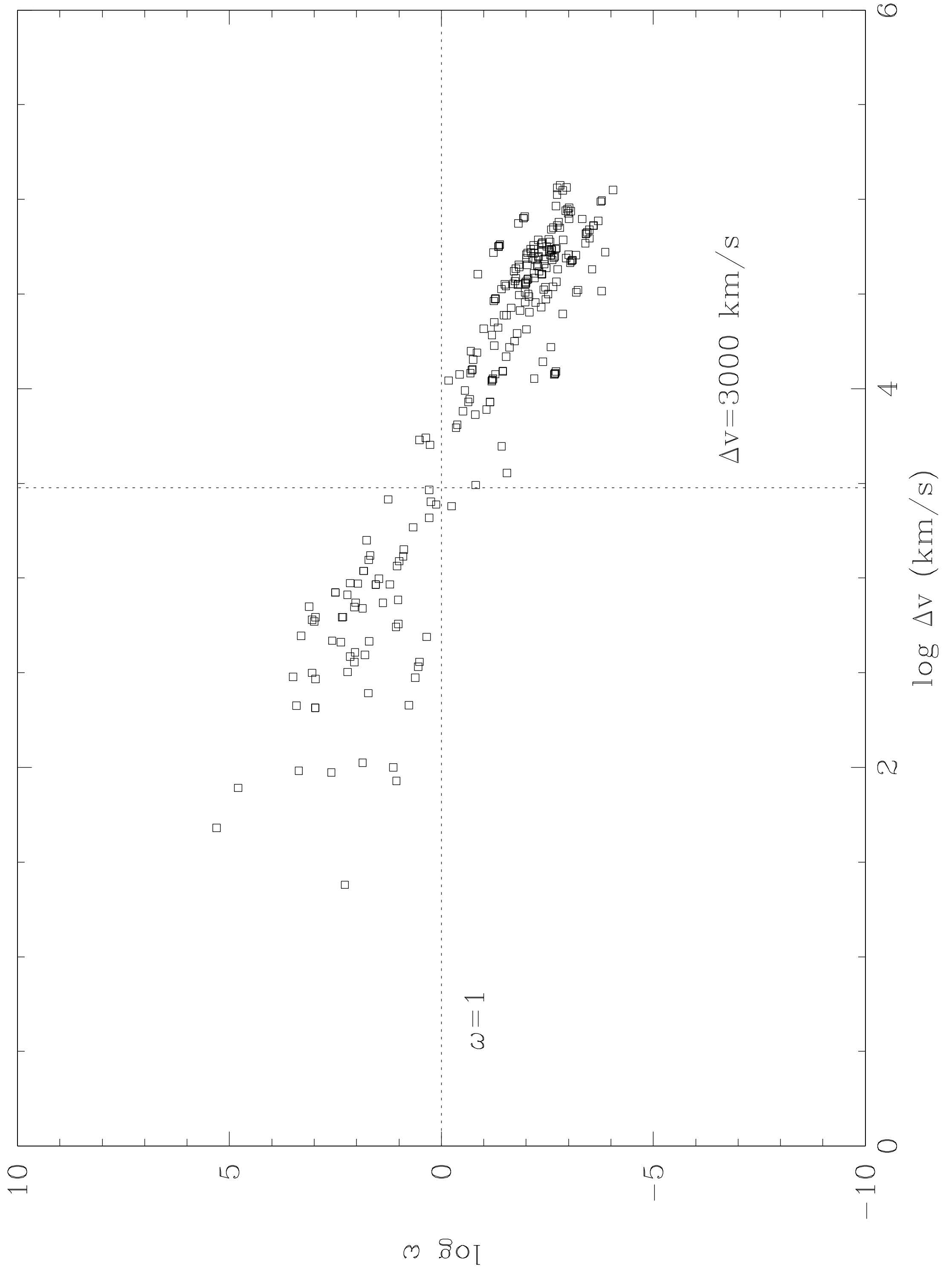
log ε
10
5
0
−5
−10
log Δv (km/s)
0
2
4
6
ω=1
Δv=3000 km/s

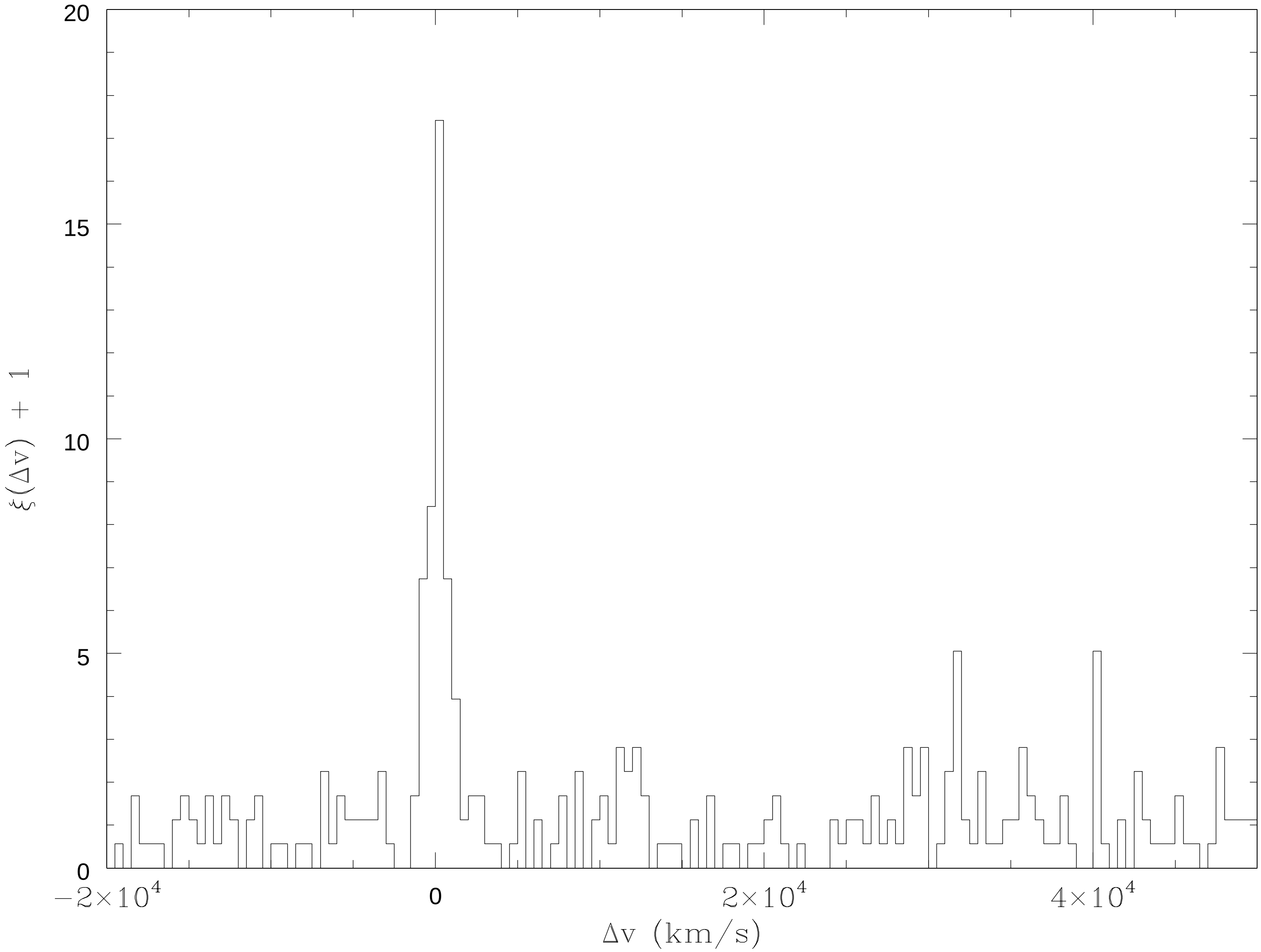
20
15
10
5
0
ξ(Δv) + 1
−2×10⁴
0
2×10⁴
4×10⁴
Δv (km/s)